6th European Conference on Computational Mechanics (ECCM 6)
7th European Conference on Computational Fluid Dynamics (ECFD 7)
11 – 15 June 2018, Glasgow, UK

INFLUENCE OF VISCOUS DAMPERS UNCERTAINTIES ON THE SEISMIC RISK OF A LOW-RISE STEEL BUILDING

F. SCOZZESE[1], A. DALL'ASTA[2] AND E. TUBALDI[3]

[1] Polytechnic University of Marche, Department of Civil and Building Engineering and Architecture
Via Brecce Bianche Ancona (AN), Italy
fabrizioscozzese@gmail.com

[2] School of Architecture and Design, University of Camerino
Viale della Rimembranza, 63100 Ascoli Piceno (AP), Italy.
andrea.dallasta@unicam.it

[3] University of Strathclyde
16 Richmond St., G1 1XQ Glasgow, United Kingdom
etubaldi@gmail.com

Key words: Reliability, Seismic Risk, IM-based Approach, Damper Uncertainties.

Abstract. Fluid viscous dampers are widely employed to control and enhance the seismic response of structural systems. However, the reliability of these devices may be significantly affected by the uncertainty inherent to the manufacturing process, which might lead the dampers to respond in an unexpected way. The main international codes acknowledge the aforementioned issue and provide some acceptance criteria requiring that the response of prototype tests, generally expressed in terms of force-velocity relation, does not deviate from the nominal design condition by more than a tolerance. However, no prescriptions or limits are imposed on the viscous damper constitutive parameters (viscous coefficient c and velocity exponent α), whose admissible ranges of variability are unknown. The present paper aims to investigate how the seismic performance of a structural system, described in terms of mean annual rates of exceedance of the relevant response parameters, is affected by the uncertainty of damper properties. The investigation is carried out on a benchmark case study consisting of a low-rise steel moment-resisting frame building equipped with a set of linear and nonlinear viscous dampers, designed to achieve the same deterministic target performance for a reference seismic scenario. The study results show that the damper properties variability affects differently the various response parameters considered, and that in some cases significant seismic demand amplifications can be observed.

1. INTRODUCTION

Fluid viscous dampers (FVDs) are widely employed to control and enhance the seismic response of structural systems. Some recent studies [1,2] proved their effectiveness in mitigating the seismic risk of structural systems when the seismic input uncertainties are explicitly accounted for. However, the reliability of these devices may be significantly affected by the uncertainty inherent to the manufacturing process, which might lead the dampers to respond in an unexpected way.

The main international codes (ASCE/SEI-7, ASCE/SEI 41-13, EN 15129) [3–5] acknowledge the aforementioned issue and provide acceptance/tolerance criteria, requiring that the response of prototype tests, generally expressed in terms of force-velocity relation, does not deviate from the nominal design condition by more than a tolerance quantity. However, no prescriptions or limits are imposed on the viscous damper constitutive parameters (viscous coefficient c and velocity exponent α), whose admissible ranges of variability are unknown.

The studies conducted on this specific aspect are very scarce. Lavan and Avishur 2013 [6] investigated the sensitivity of the response of linearly damped frames to uncertainty in structural and damping properties, the latter accounted through a coefficient of variation equal to 5% on the dampers viscous coefficients only (α deterministically fixed at its design value). Dall'Asta et al. 2017 [7] analysed, via Subset Simulation, the seismic response sensitivity of S-DoF systems equipped with linear and nonlinear viscous devices to variable c and α, observing a non-negligible influence of the α exponent variability.

The present paper aims to extend this work [7] by evaluating the influence of code-complying damper property variations on the performance of a low-rise steel moment-resisting frame. The frame is equipped with a set of linear (α=1.0) and nonlinear (α=0.3) viscous dampers, designed to achieve the same deterministic target performance for a reference seismic scenario, and the investigation is carried out by considering two different cases of damper uncertainties: 1) variable c and fixed α, equal to the nominal design value; 2) combined variation of c and α. The seismic performance is described by means of demand hazard curves, reporting the mean annual frequency (MAF) of exceedance for the most relevant engineering demand parameters (EDPs), and an efficient hybrid probabilistic approach is used to achieve accurate estimates of these MAFs with a small number of simulations.

2. METHODOLOGY

2.1 Seismic performance assessment

The seismic design and assessment of structures aims at ensuring that the probability of having an unsatisfactory performance (often referred to as failure) is lower than a reference acceptable level, whose value is prefixed by seismic codes and can be tailored to the type of structure at hand, its function, and the consequences of failure (ASCE 7-10; Eurocode-0**Errore. L'origine riferimento non è stata trovata.**; Probabilistic Model Code 2000) [8,9,3]. With reference to ordinary civil structures, different limit states and levels of the allowed exceedance probability are introduced to control the performance. Conventional thresholds are specified for these limit states and the mean annual frequencies (MAFs) of exceedance approximately vary from $1 \cdot 10^{-2}$ 1/year for serviceability limit states to $1\text{-}2 \cdot 10^{-3}$ 1/year for ultimate limit states [8,9,3], while safety checks against collapse should be oriented to ensure a mean annual failure rate lower than 10^{-5}-10^{-6} [11,28].

In general, the seismic structural performance is evaluated by monitoring a set of EDPs relevant to the system at hand, and the seismic check aims to verify that the mean annual frequency (MAF) $\nu_{EDP}(d_f)$ of exceeding a prefixed threshold value d_f is lower than an acceptable limit ν_0 (depending on the particular limit state or performance condition, as discussed above). Design codes [8,9,3] and practical assessment procedures follow an "intensity-based assessment approach" [10], aiming at satisfying the aforementioned reliability

condition in an indirect and simplified way, avoiding probabilistic analyses. For this purpose, a conventional seismic response measure d^* is evaluated, via structural analysis, under a seismic input with assigned intensity, and then it is verified that $d^* < d_f$. Different threshold values of d_f, each associated to a performance objective, are coupled with the various intensity levels.

A more rigorous performance assessment should consider explicitly the seismic demand hazard function, $\nu_{EDP}(d)$, expressing the MAF of exceeding different values d of the global and local EDP relevant to the performance of the analyzed system [10]. Obviously, in the evaluation of $\nu_{EDP}(d)$, all the sources of uncertainty involved in the problem shall be accounted for. In this regard, it may be convenient to consider two separate vectors for describing these uncertainties: $\boldsymbol{X} \in \boldsymbol{\Omega}$ is the vector collecting the random variables representing the ground motion and the structural system uncertainties, which can be described by assigning a probability density function, and $\boldsymbol{\theta} \in \Gamma$ is the vector of all the other parameters affecting the system performance (i.e., dampers' properties uncertainties), but for which a probabilistic model is not available. The corresponding nominal values of $\boldsymbol{\theta}$ are hereafter denoted as $\boldsymbol{\theta}_0$.

Denoting with $d(\boldsymbol{x}|\boldsymbol{\theta})$ the generic demand conditional to a given combination of model parameters $\boldsymbol{\theta}$, it is possible to evaluate explicitly how $\boldsymbol{\theta}$ affects the seismic demand hazard function $\nu_{EDP}(d|\boldsymbol{\theta})$ by solving the reliability integral,

$$\nu_{EDP}(d|\boldsymbol{\theta}) = \nu_{min} \int_{\boldsymbol{\Omega}} I_d(\boldsymbol{x}|\boldsymbol{\theta})\, p_{\boldsymbol{X}}(\boldsymbol{x}) dx \tag{1}$$

in which $p_X(\boldsymbol{x})$ is the joint probability density function (PDF) of $\mathbf{X}$, and $I_d(\boldsymbol{x}|\boldsymbol{\theta})$ is an indicator function, such that $I_d = 1$ if $d(\boldsymbol{x}|\boldsymbol{\theta}) > d^*$, otherwise $I_d = 0$. The multiplicative term ν_{min} is the MAF of occurrence of a seismic event of any significant magnitude [11].

2.2 Hybrid reliability approach for seismic demand estimation

Monte Carlo techniques [12–14] could be employed for solving the integral of Eq. (1), but this type of approach is generally computationally expensive. An efficient probabilistic approach, denoted hereinafter as hybrid, is employed here to achieve accurate estimates of the $\nu_{EDP}(d^*|\boldsymbol{\theta})$ while limiting the number of simulations. For this purpose, a conditional probabilistic technique [10] is used to evaluate the seismic demand at different seismic intensity levels. More precisely, a stochastic ground motion model is considered, and Subset Simulation (SS) [14] is employed to derive the IM hazard curve, $\nu_{IM}(im)$, up to very small rates of exceedances. SS also provides a set of stochastic ground motion samples conditional to different, non-overlapping IM intervals, which are considered to build the conditional seismic demand model via multiple-stripe analysis (MSA) [15]. This demand model, represented by $G_{D|IM}(d|\boldsymbol{\theta}, im)$, expresses the probability of exceeding the demand value d, conditional to the seismic intensity im, and can be estimated via an empirical method, i.e., by counting the fraction of samples larger than d for each IM level. The MAF $\nu_{EDP}(d^*|\boldsymbol{\theta})$ can then be evaluated as

$$\nu_{EDP}(d^*|\boldsymbol{\theta}) = \int_{IM} G_{D|IM}(d^*|\boldsymbol{\theta}, im)\, |d\nu_{IM}| \tag{2}$$

where the integral is computed numerically by employing a trapezoidal rule.

It is worth mentioning that this hybrid approach has been recently used in [16] for testing different ground motion selection methods. However, differently from that work, employing a

pure Monte Carlo approach for the simulations, in this study the more efficient Subset Simulation [14] is used, thus reducing further the computational cost of analysis.

3. VISCOUS DAMPERS WITH VARIABLE PROPERTIES

3.1 Overview

The force-velocity constitutive law of FVDs can be described through the following relationship [17–19]:

$$F_d(v) = c|v|^{\alpha} sgn(v) \tag{3}$$

where v is the velocity between the device's ends, F_d is the damper resisting force, $|v|$ is the absolute value of v, *sgn* is the sign operator, c and α are two constitutive parameters: the former is a multiplicative factor, while the latter describes the damper nonlinear behaviour.

The main international seismic codes [3–5] acknowledge that the manufacturing process is characterized by some uncertainty affecting the viscous constitutive parameters, whose actual values might differ from the nominal ones used in the design. To cope with such uncertainty, acceptance criteria are introduced. In particular, the ASCE/SEI 41-13 [4]**Errore. L'origine riferimento non è stata trovata.** and the European code EN 15129 [5] require that the maximum experimental force shown by the tested damper (subjected to harmonic displacement time-histories), $F_d(v)$, deviates from the expected (design) value, $F_d^*(v)$, by no more than a tolerance value p within a range of velocities v spanning from zero to the maximum design one v^*. This requirement can be formulated in terms of the following inequality,

$$(1-p)F_d(v) \le F_d(v) \le (1+p)F_d(v), \qquad v \le v \le v^* \tag{4}$$

where p = 15% according to the abovementioned seismic standards. The safety check should be coherently carried out by employing a lower/upper bound approach, considering the worst conditions compatible with the acceptance criteria.

The application proposed in this paper, which can be viewed as an extension of a previous work of the same authors [20] to the case of more realistic structural models including multiple devices, aims at investigating the influence of the variability of the viscous damper properties, including that of α, on the seismic risk. To this aim, by denoting the viscous constitutive properties of n fluid viscous dampers as $\boldsymbol{c} = [c_1, \ldots, c_n]$ and $\boldsymbol{\alpha} = [\alpha_1, \ldots, \alpha_n]$, it is possible to consider two rules of variation complying with the tolerances prescribed by the code, as described below in detail.

3.2 Code-complying dampers properties variations

The simplest case considered corresponds to variable viscous coefficients $\boldsymbol{c}$ and fixed velocity exponents $\boldsymbol{\alpha}$, the latter assumed equal to the corresponding nominal values $\boldsymbol{\alpha}_0$. Viscous coefficients are allowed to deviate from the nominal values $\boldsymbol{c}_0$ while satisfying the inequality constraint of Eq. (4), which can be also expressed as in Eq. (3) because the variations of $\boldsymbol{c}$ provide a homogeneous effect on the damper response for the whole range of velocities, with force variations equal to the viscous coefficient variations,

$$-0.85c_{0,i} \le c_i \le 1.15c_{0,i} \; (i = 1, \ldots, n) \tag{5}$$

Alternatively, both $\boldsymbol{c}$ and $\boldsymbol{\alpha}$ might be assumed to vary while satisfying Eq. (4). In this case, the link between the dampers force variations and the perturbed viscous parameters is not straightforward, and joint variations ($\hat{\boldsymbol{\alpha}}$, $\hat{\boldsymbol{c}}$) of the constitutive parameters, such that $\boldsymbol{\alpha} = \boldsymbol{\alpha}_0 + \hat{\boldsymbol{\alpha}}$ and $\boldsymbol{c} = \boldsymbol{c}_0 + \hat{\boldsymbol{c}}$, must be considered. The constraint of Eq. (4) can be rewritten as follows,

$$\left|\left(c_{0,i} + \hat{c}_i\right)v^{\left(\alpha_{0,i}+\hat{\alpha}_i\right)} - c_{0,i}v^{\alpha_{0,i}}\right| \leq 0.15c_{0,i}v^{\alpha_{0,i}}, \forall\ 0 \leq v \leq v^*\ \ (i = 1, \dots, n) \qquad (6)$$

in which the perturbed parameters have been spelt out.

For sake of clarity, Fig. 1(a) and (b) show, with black solid line, the normalized force-velocity relations corresponding to respectively a linear and a nonlinear damper (b), obtained for the design nominal parameters (α_0, c_0). On the same figure, the upper and lower bounds of the allowed response variability are also shown with red solid lines, corresponding to the case of viscous coefficient variations $\hat{c} = +/-15\%$ and $\hat{\alpha} = 0$. Moreover, the varied response curves obtained for two specific pairs of perturbed values ($\hat{\alpha}$, $\hat{c}$) are superimposed: the dashed blue curve represents the maximum admissible positive variation of the exponent α, corresponding to the condition in which the response variation attains the upper bound value (i.e., $F_d/\ F_d^* = 1.15$) at the design velocity (i.e., $v/\ v^*=1$); the dotted blue curve represents the maximum admissible negative variation of the exponent α, corresponding to the condition in which the response variation attain the lower bound value (i.e., $F_d/\ F_d^* = 0.85$) at the design velocity (i.e., $v/\ v^*=1$).

The perturbed cases discussed above comply with the tolerances for velocity values lower than the design one (i.e., $v/\ v^* < 1$), as required by the codes. However, for velocity values beyond the design one (i.e., $v/\ v^* > 1$), the perturbed force attains values outside the upper/lower bounds, and the specific trend depends on the sign of $\hat{\alpha}$, which governs the rate of change of the nonlinear response with non-homogeneous effects along the range of velocities.

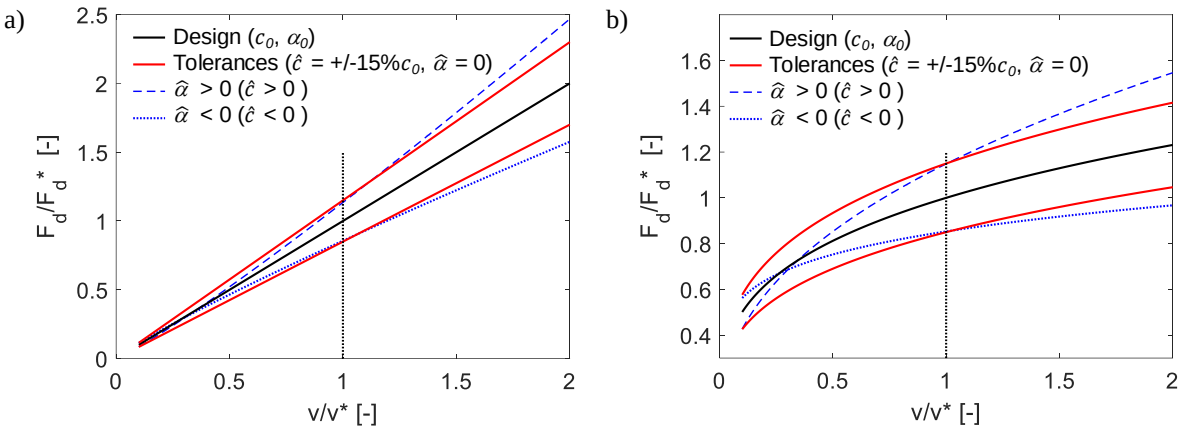

Fig. 1: FVD's force response for code-complying damper parameters variations: a) α_0 =1.0, and b) α_0 =0. 3.

4. BENCHMARK CASE STUDY AND DAMPERS DESIGN

4.1 Case study and dampers design

The case study consists of a 3-storey steel moment-resisting (MR) frame building, designed within the SAC Phase II Steel Project, and widely used as benchmark structure in [21,22,2,23]. The structural system was designed to conform to local code requirements of California region.

It consists of perimeter moment-resisting frames and internal gravity frames with shear connections, while the structural model for analysis purposes is a two-dimensional frame representing one half of the structure in the north–south direction. The main geometrical details are shown in Fig. 2, while further details can be found in [22].

The finite element model of the system is developed in OpenSees [24] by following a distributed plasticity approach. An elastic P-delta column is introduced to account for the nonlinear geometrical effects induced by gravity loads, corresponding to both the inner frames and, not explicitly modelled, and the perimeter frame, explicitly modelled. A large displacement (small strain) analysis is performed. The estimated first three vibration periods T_1=0.995 s, T_2=0.325 s, and T_3=0.173 s, are in good agreement with the values observed in [21,22,2].

4.2 Seismic scenario and intensity measure

The Atkinson-Silva (2000) [25] source-based ground motion model for California region is used to characterize the seismic hazard at the site of the building. Ground motion samples can be generated using this model in combination with the stochastic simulation method of Boore (2003) [26]. The seismic scenario at the site is described through the following two seismological parameters, modelled as random variables: the moment magnitude M is characterized by the Gutenberg-Richter PDF $f_M(m)$ bounded within the interval [5, 8] and with parameter $\beta=2.303$; the epicentral distance R is modelled according to the PDF $f_R(r)$ under the hypothesis of equal likelihood of seismic occurrence anywhere within a distance from the site r_{max} = 50 km, beyond which the seismic effects are assumed to become negligible. The soil condition is deterministically defined by the scalar value V_{S30} = 310 m/s [27]. Further details about the other ground motion model parameters not reported here can be found in [20]**Errore. L'origine riferimento non è stata trovata.**. The ground motion record-to-record variability is simulated by means of a Gaussian normal vector-valued function, by adding a lognormal random variable ε_{mod} as proposed by Jalayer and Beck (2008) [28] to increase the otherwise low record-to-record casualness.

The spectral acceleration at the fundamental period T_1 = 1.0 s, $S_a(T_1)$, is assumed as IM, and the corresponding hazard curve is provided by a single-run of Subset Simulation, performed with 20 simulation levels, each having a target intermediate exceedance probability p_0 = 0.5, and N=500 samples per level. Among the N=500 ground motion time-series generated at each simulation level, a subset of 20 samples is considered for performing MSA. It is noteworthy that number of simulation levels has been defined based on a preliminary study, performed by considering different choices for the discretization of the IM range and for the numbers of accelerograms to be considered at each IM interval. Based on this study, it was concluded that a hybrid reliability analysis with 20 stripes and 20 ground motion samples conditional to the central values of the partitioned IM hazard curve allows to obtain results comparable in terms of accuracy to those provided by multiple Subset Simulations, for which an average of 20 independent runs, corresponding to a total of 24000 simulations, is considered.

4.3 Performance criteria and dampers design

The dampers are designed to achieve an enhanced building performance level according to ASCE/SEI 41-13 [4], consisting of meeting the immediate occupancy requirements

(performance level 1-B) at the BSE-2E seismic hazard level (i.e., with probability of exceedance equal to 5% in 50 years, corresponding to the annual rate of exceeding $\nu_0 = 0.001$).

The dampers are placed into the structural frame (Fig. 2) connected in series to steel supporting braces, and two different cases are studied: linear viscous dampers ($\alpha_0 = 1.0$) and nonlinear ($\alpha_0 = 0.3$) viscous dampers. The structural performance is described by the interstory maximum drift, whose limit value at the Immediate Occupancy Limit State is assumed equal to 0.01 according to FEMA-350 [29] for low-rise ordinary moment-resisting steel buildings.

Following a deterministic design approach, commonly employed in practice, the damper viscous coefficients $c_{0,i}$ (i = 1, 2, 3 floor levels) are calibrated to control the mean value of the maximum interstory drift demand (μ_{drift_max}), evaluated for a set of 7 accelerograms whose intensity, defined in terms of IM= $S_a(T_1)$, is consistent with the reference hazard level (i.e., with $\nu_0 = 0.001\text{yr}^{-1}$). The IM value corresponding to the exceedance frequency considered for the design is equal to IM(ν_0) = $S_a(T_1)$ = 0.63g. The subset of 7 simulated ground motion time-histories is selected from the set of samples stored during execution of Subset Simulation, and the selection criteria is such that it satisfies (without scaling) the spectrum compatibility at the building's first period T_1 = 1.0s. The target performance, achieved for both the linear and nonlinear dampers case, is equal to μ_{drift_max} = 0.0097rad < 0.01rad, corresponding to a 40% reduction with respect to the bare frame performance.

Assuming a S275 steel grade, the supporting braces are designed to withstand (with no buckling) an amplified damper force according to the following expression,

$$F_b = F_d(2\mu_{vel,max}) = c_0|2\mu_{vel,max}|^{\alpha} \tag{7}$$

corresponding to the force provided by the damper at a velocity value twice the mean maximum velocity $\mu_{vel,max}$ observed under the set of 7 ground motions conditional to IM(ν_0).

Among the several methods available [30] for distributing the dampers at the various storeys, a distribution of $c_{0,i}$ proportional to the normalized shear profile (i.e., from the top below, 0.54, 0.86, 1.00) of the first mode is considered in this study. The nominal properties of the viscous coefficients and axial stiffness of the steel braces are reported in Table 1.

The performance of the system with added dampers is evaluated by monitoring the following EDPs: the maximum interstory drift among the storeys, edp_{Drift}; the maximum absolute base-shear brought by the frame only, edp_{Vb_Frame}; the maximum absolute acceleration among the various floors, edp_{Acc}; the maximum absolute force and strokes among the dampers, respectively, $edp_{Fd\ Di}$ and $edp_{Stroke\ Di}$ (accounting for devices' cost, size and failure). The maximum velocities experience by dampers, edp_{Vel_Di}, are also monitored.

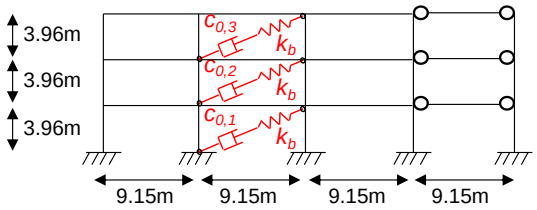

Fig. 2: Structural model and FVDs placement.

Table 1: Damper parameters and brace stiffness with linear and nonlinear dampers.

$c_{0,1}$ [$s^{\alpha+2}/m^{\alpha+1}$]	$c_{0,2}$ [$s^{\alpha+2}/m^{\alpha+1}$]	$c_{0,3}$ [$s^{\alpha+2}/m^{\alpha+1}$]	k_b [kN/mm]

α_0 =1.0	11000	9460	5940	640.23
α_0 =0.3	4000	3440	2160	409.75

5. HAZARD CURVES FOR DAMPERS WITH NOMINAL PROPERTIES

This section shows and compares the seismic performances of the buildings equipped with linear and nonlinear dampers with nominal properties ($\alpha_{0,i}$, $c_{0,i}$). In particular, the demand hazard curves are estimated via MSA for all of the relevant EDPs, but due to space constraints only some responses (i.e., drift, accelerations, stroke and force of the damper at the first-floor) are shown in Fig. 3. The curves related to the system equipped with linear dampers (red solid line) and nonlinear dampers (blue solid line) are plotted together with the corresponding reference performance points, having the coordinates $\{d^*, \nu_0(d^*)\}$ and illustrated with red and blue circles for, respectively, linear and nonlinear dampers. The makers corresponding to the design response values amplified according to ASCE/SEI 41-13 [4] are also shown, using red and blue diamonds for, respectively, linear and nonlinear dampers. It is recalled, indeed, that the amplification rules suggested in ASCE/SEI 41-13 are as expressed in Eq. (7) for what concerns the forces (i.e., by assuming a damper velocity twice the design value), while the strokes are required to be amplified by a factor 2.

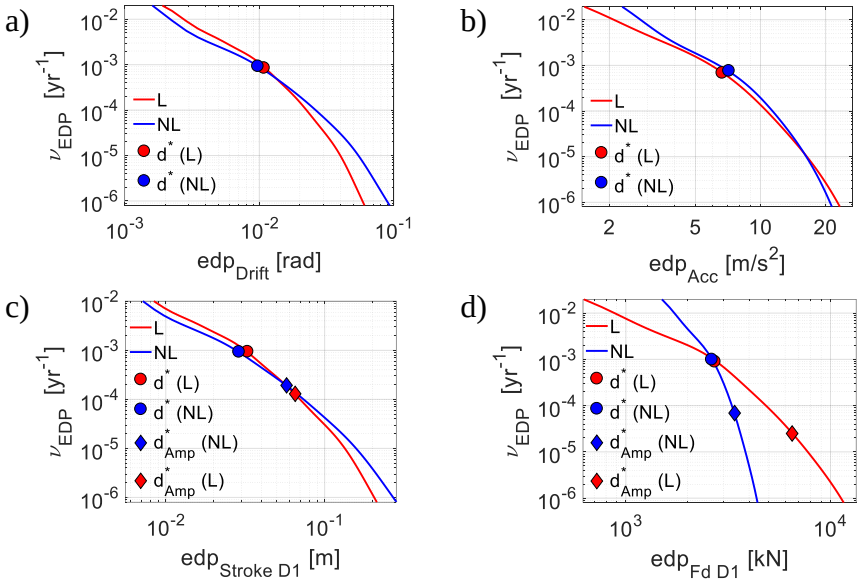

Fig. 3: Demand hazard curves for dampers with nominal properties.

By analysing the results (including those not reported in Fig. 3), it can be observed that the reference MAF of exceedance is around 10^{-3} (see red and blue circles in the charts) for all the EDPs and types of dampers. However, the EDPs' hazard curves show different trends between linear and nonlinear dampers by moving above or below the reference MAF value. In particular, it is found that:

- The structural response in terms of drift (Fig. 3a), dampers' velocity and strokes (Fig. 3c) is higher in the building with linear dampers within the range of MAFs $\nu_{EDP} > 10^{-3}$ (i.e., more frequent events), while the trend is inverted by moving toward the rarer events region with $\nu_{EDP} < 10^{-3}$. This implies a better performance of linear dampers for

ν_{EDP} <10^{-3} (reference design MAF), and a worse performance for ν_{EDP} >10^{-3}.

- The hazard curves of the dampers' forces (Fig. 3d) and the frame base-shear follow an inverted trend, in which the response of the building with nonlinear dampers is higher within the range of MAFs ν_{EDP} >10^{-3}, and lower for ν_{EDP} <10^{-3}.
- The maximum absolute acceleration (Fig. 3b) is higher in the building with nonlinear dampers within the range of MAFs ν_{EDP} >10^{-5} and lower for ν_{EDP} <10^{-5}.

Furthermore, it is worth to note that the amplification rules provided by ASCE/SEI 41-13 for both the stroke and force of dampers do not lead to homogenous reliability levels:

- The amplified design force (Fig. 3d) is more likely to be exceeded by the nonlinear dampers (ν_{EDP} =8.819x10^{-5} yr^{-1} in average) than by the linear ones (ν_{EDP} =3.479x10^{-5}).
- The same results are observed for the amplified design stroke (Fig. 3c), which is more likely exceeded by the nonlinear dampers (with an average ν_{EDP} = 1.996x10^{-4} yr^{-1}) than by the linear ones (with an average ν_{EDP} =1.136x10^{-4}).
- The MAF of the amplified stroke is on average higher than that of the damper force.

The results discussed above are in agreement with the outcomes of previous studies [20,21], and confirm the need of improving the simplified approach provided by the codes, which does not ensure the same reliability levels for dampers with different exponent α.

6. EFFECT OF VARIABLE VISCOUS PROPERTIES

6.1 Demand hazard curves for dampers with varied viscous properties

This section analyses the influence of dampers with variable viscous properties. The following two pairs of perturbed conditions are investigated (Fig. 1): 1) dampers with viscous coefficients equal to the upper and lower limit values allowed by the code, i.e., corresponding to $\hat{c}_i = +/-15\%c_{0,i}$ and $\hat{\alpha}_i = 0$; 2) dampers with the maximum admissible positive and negative variations of the exponent α (and related viscous coefficient), corresponding to the condition in which the damper force variation attains, respectively, the upper and lower bound values (i.e., $F_d/\ F_d^*$ = 1.15 and $F_d/\ F_d^*$ = 0.85) at the design velocity (i.e., $v/\ v^*$ = 1). To be more specific, each of the three dampers placed in the building has a specific value of design velocity v^*, hence the pairs of varied constitutive parameters vary from a damper to another. However, because the values of the design velocities are very similar for the various dampers, a unique pair of perturbed parameters is assumed, for each damper type (linear or nonlinear). In particular, the maximum design velocity experienced by the dampers at different floors is considered, i.e., 0.314 m/s and 0.313 m/s for, respectively, linear and nonlinear dampers. Thus, in the case of linear dampers the pairs of varied parameters correspond to the variations $\{\hat{c}_i = +31.7\%c_{0,i};\ \hat{\alpha}_i = +12.1\%\alpha_{0,i}\}$ and $\{\hat{c}_i = -26.2\%c_{0,i};\ \hat{\alpha}_i = -12.1\%\alpha_{0,i}\}$, while in the case of nonlinear dampers they correspond to the variations $\{\hat{c}_i = +32.8\%c_{0,i};\ \hat{\alpha}_i = +39.3\%\alpha_{0,i}\}$ and $\{\hat{c}_i = -25.9\%c_{0,i};\ \hat{\alpha}_i = -39.3\%\alpha_{0,i}\}$.

The influence on the seismic performance of these variations of the damper properties is assessed by monitoring the response at the following three MAF levels: 10^{-2}, 10^{-3}, and 10^{-6}, which are approximately representative of, respectively, the serviceability limit state (SLS), the ultimate limit state (ULS), and the failure conditions. At each of these MAF levels, the percentage variation of the generic seismic demand parameter is computed through Eq. (8), in which d_{var} is the EDP value for perturbed parameters, and d_0 is the one for nominal conditions.

$$\Delta d_{max}(\nu_{EDP}) = 100\frac{d_{var}(\nu_{EDP}) - d_0(\nu_{EDP})}{d_0(\nu_{EDP})} \tag{8}$$

Table 2: Percentage performance demand variations at the MAF level $\nu_{EDP} = 10^{-2}$.

	$\hat{c} = +15\%$ ($\hat{\alpha} = 0$)		$\hat{c} = -15\%$ ($\hat{\alpha} = 0$)		$\hat{\alpha} > 0$ and $\hat{c} > 0$		$\hat{\alpha} < 0$ and $\hat{c} < 0$	
Damper type	*L*	*NL*	*L*	*NL*	*L*	*NL*	*L*	*NL*
edp_{Drift}	0.00	0.00	0.00	0.00	-21.73	0.00	**21.73**	0.00
edp_{Vb_Frame}	7.67	11.98	-7.67	-11.98	**15.34**	**23.96**	-11.50	-19.97
edp_{Acc}	0.00	6.88	0.00	-6.88	0.00	**13.76**	0.00	-6.88
$edp_{Fd\_dampers}$	14.12	7.10	-14.12	-14.20	**14.12**	**21.31**	-14.12	-21.31
$edp_{Stroke\_dampers}$	-11.36	0.00	11.36	0.00	-11.36	0.00	**11.36**	**14.71**
$edp_{Vel\_dampers}$	-5.78	0.00	5.78	-4.92	-5.78	4.92	11.56	-9.85

Table 3: Percentage performance demand variations at the MAF level $\nu_{EDP} = 10^{-3}$.

	$\hat{c} = +15\%$ ($\hat{\alpha} = 0$)		$\hat{c} = -15\%$ ($\hat{\alpha} = 0$)		$\hat{\alpha} > 0$ and $\hat{c} > 0$		$\hat{\alpha} < 0$ and $\hat{c} < 0$	
Damper type	*L*	*NL*	*L*	*NL*	*L*	*NL*	*L*	*NL*
edp_{Drift}	-6.02	-6.85	6.02	**13.70**	-12.05	-13.70	12.05	**20.55**
edp_{Vb_Frame}	5.74	9.08	-6.89	-7.95	**12.63**	**19.30**	-12.63	-13.62
edp_{Acc}	0.00	0.00	0.00	0.00	**3.17**	**2.90**	0.00	0.00
$edp_{Fd\_dampers}$	9.06	14.23	-9.06	-14.23	**18.12**	**28.46**	-18.12	-23.72
$edp_{Stroke\_dampers}$	-6.10	-6.71	9.15	10.07	-12.20	-13.42	**15.24**	**16.78**
$edp_{Vel\_dampers}$	-3.75	-3.75	5.63	9.38	-7.50	-5.63	**11.26**	**15.01**

Table 4: Percentage performance demand variations at the MAF level $\nu_{EDP} = 10^{-6}$.

	$\hat{c} = +15\%$ ($\hat{\alpha} = 0$)		$\hat{c} = -15\%$ ($\hat{\alpha} = 0$)		$\hat{\alpha} > 0$ and $\hat{c} > 0$		$\hat{\alpha} < 0$ and $\hat{c} < 0$	
Damper type	*L*	*NL*	*L*	*NL*	*L*	*NL*	*L*	*NL*
edp_{Drift}	-7.48	-6.36	8.55	7.77	-13.89	-12.71	**16.03**	**14.83**
edp_{Vb_Frame}	8.33	8.77	-8.65	-8.18	**16.98**	**18.70**	-15.70	-14.61
edp_{Acc}	2.49	3.59	-1.66	-3.59	**4.98**	**8.07**	-3.32	-5.38
$edp_{Fd\_dampers}$	9.99	14.25	-11.10	-14.25	**19.98**	**31.36**	-19.98	-25.66
$edp_{Stroke\_dampers}$	-7.03	-6.41	8.66	7.83	-13.53	-12.82	**16.23**	**14.60**
$edp_{Vel\_dampers}$	-3.00	-4.76	3.49	5.12	-5.49	-8.78	**6.49**	**9.15**

Based on the results computed for both the cases of linear (L) and nonlinear (NL) dampers, reported in Table 2-Table 4 (with the highest positive variations highlighted by black solid fonts), the following conclusions can be drawn:

- For all of the MAF levels examined, the perturbed cases with ($\hat{c} = +15\%$ and $\hat{\alpha} = 0$) and ($\hat{c} > 0$ and $\hat{\alpha} > 0$) lead to negative variations of the drift, strokes and damper velocity demand, while yield positive variations on the frame base-shears, damper forces and absolute accelerations.
- The highest variations are observed for combined perturbations of the parameters ($\hat{c} \neq 0$ and $\hat{\alpha} \neq 0$), whereas the EDPs are generally less sensitive to variations of *c* only.
- A clear trend among the MAF levels cannot be identified for most of the EDPs, even

though the damper force sensitivity to the parameters perturbations increases by moving towards rarer hazard levels, i.e., passing from SLS to the collapse region.

- The maximum increments reached by the damper strokes are higher than 16% in both linear and nonlinear dampers when $\hat{c} < 0$ and $\hat{\alpha} < 0$, while the maximum increments reached by the damper forces are around 31% and 20% for, respectively, nonlinear and linear dampers when $\hat{c} > 0$ and $\hat{\alpha} > 0$.

Results discussed thus far are consistent with the outcomes obtained in [20] by considering a linear SDOF system with period T=1.0s.

7. CONCLUSIONS

This paper analyses the influence of code-complying tolerances of viscous damper properties on the probabilistic performance of a low-rise steel moment-resisting frame building equipped with a set of linear (α=1.0) and nonlinear (α=0.3) viscous dampers.

The study results show that the damper properties variability affects differently the various response parameters considered, and in some cases significant seismic demand amplifications are observed with respect to the case with dampers with nominal properties. In light of this, should these results be confirmed in future studies, it may be advisable to improve the reliability factors currently provided by the codes in order to account for dampers uncertainties.

ACKNOWLEDGEMENTS

This study was sponsored by the Italian Department of Civil Protection within the Reluis-DPC Projects 2014-2018. The authors gratefully acknowledge this financial support.

REFERENCES

[1] Seo C.Y., Karavasilis T.L., Ricles J.M., Sause R. Seismic performance and probabilistic collapse resistance assessment of steel moment resisting frames with fluid viscous dampers. *Earthq Eng Struct Dyn* (2014) **43**:2135–2154. doi:10.1002/eqe.2440.

[2] Barroso L.R., Winterstein S. Probabilistic seismic demand analysis of controlled steel moment-resisting frame structures. *Earthq Eng Struct Dyn* (2002) **31**:2049–2066.

[3] ASCE/SEI 7-10: Minimum design loads for buildings and other structures. 2010.

[4] ASCE 41-13: Seismic Evaluation and Retrofit Rehabilitation of Existing Buildings 2014.

[5] European Committee for Standardization. EN 15129:2010 - Antiseismic devices. 2010.

[6] Lavan O., Avishur M. Seismic behavior of viscously damped yielding frames under structural and damping uncertainties. *Bull Earthq Eng* (2013) **11**:2309–2332.

[7] Dall'Asta A., Scozzese F., Ragni L., Tubaldi E. Effect of the damper property variability on the seismic reliability of linear systems equipped with viscous dampers. *Bull Earthq Eng (*2017) **15**:5025–5053. doi:10.1007/s10518-017-0169-8.

[8] Jcss. Probabilistic Model Code - Part 1. Struct Saf 2001:65.

[9] Eurocode 0 - Basis of structural design. En 2002;3:89. doi:10.1680/cien.144.6.8.40609.

[10] Bradley B.A. A comparison of intensity-based demand distributions and the seismic demand hazard for seismic performance assessment. *Earthq Eng Struct Dyn* (2013) **42**:2235–2253. doi:10.1002/eqe.2322.

[11] Altieri D., Tubaldi E., De Angelis M., Patelli E., Dall'Asta A. Reliability-based optimal

design of nonlinear viscous dampers for the seismic protection of structural systems. *Bull Earthq Eng* (2018) **16**:963–82. doi:10.1007/s10518-017-0233-4.

[12] Jayaram N., Baker J.W. Efficient sampling and data reduction techniques for probabilistic seismic lifeline risk assessment. E*arthq Eng Struct Dyn* (2010) **39**(10), 1109-1131.doi:10.1002/eqe.988.

[13] Rubinstein R., Kroese D. *Simulation and the Monte Carlo method*. 2016.

[14] Au S.K., Beck J.L. Subset Simulation and its Application to Seismic Risk Based on Dynamic Analysis. *J Eng Mech* (2003) **129**:901–917.

[15] Baker J., Cornell C. Vector-valued ground motion intensity measures for probabilistic seismic demand analysis. PEER, University of California 2006.

[16] Bradley B.A., Burks L.S., Baker J.W. Ground motion selection for simulation-based seismic hazard and structural reliability assessment. *Earthq Eng Struct Dyn* (2015) **44**:2321–2340. doi:10.1002/eqe.2588.

[17] Constantinou M., Symans M. Experimental and analytical investigation of seismic response of structures with supplemental fluid viscous dampers 1992.

[18] Castellano M.G., Borella R., Infanti S. Experimental characterization of nonlinear fluid viscous dampers according to the New European Standard. 5th Eur Conf Struct Control 2012:1–8.

[19] Symans M.D., Constantinou M.C. Passive Fluid Viscous Damping Systems for Seismic Energy Dissipation. *J Earthq Technol* (1998) **35**:185–206.

[20] Dall'Asta A., Scozzese F., Ragni L., Tubaldi E. Effect of the damper property variability on the seismic reliability of linear systems equipped with viscous dampers. *Bull Earthq Eng* (2017) **15**:5025–5053. doi:10.1007/s10518-017-0169-8.

[21] Dall'asta A., Tubaldi E., Ragni L. Influence of the nonlinear behavior of viscous dampers on the seismic demand hazard of building frames. *Earthq Eng Struct Dyn* (2016) **45**:149–169. doi:10.1002/eqe.2623.

[22] Ohtori Y., Christenson R.E., Spencer B.F., Dyke S.J. Benchmark Control Problems for Seismically Excited Nonlinear Buildings. *J Eng Mech* (2004) **130**:366–85.

[23] Gupta A., Krawinkler H. Seismic Demands for Performance Evaluation of Steel Moment Resisting Frame Structures. Dr Diss Stanford Univ 1999:1–379.

[24] Mazzoni S., Mckenna F., Scott M.H., Fenves G.L. The Open System for Earthquake Engineering Simulation (OpenSEES) User Command-Language Manual (2006).

[25] Atkinson G.M., Silva W. Stochastic modeling of California ground motions. *Bull Seismol Soc Am* (2000) **90**:255–74. doi:10.1785/0119990064.

[26] Boore, D.M. Simulation of ground motion using the stochastic method. *Pure and applied geophysics* (2003) **160**(3-4), 635-676.

[27] Boore D.M., Joyner W.B. Site amplifications for generic rock sites. *Bull Seismol Soc Am* (1997) **87**:327–41.

[28] Jalayer F., Beck J.L. Effects of two alternative representations of ground-motion uncertainty on probabilistic seismic demand assessment of structures. *Earthq Eng Struct Dyn* (2008) **37**:61–79. doi:10.1002/eqe.745.

[29] FEMA-350: Recommended seismic design criteria for new steel moment-frame buildings. Washington DC: 2000.

[30] Whittle J.K., Williams M.S., Karavasilis T.L., Blakeborough A. A comparison of viscous damper placement methods for improving seismic building design. *J Earthq Eng* (2012)

16:540–560. doi:10.1080/13632469.2011.653864.